# APPLICATION OF AN AUTOMATIC CLOUD TRACKING TECHNIQUE TO METEOSAT WATER VAPOR AND INFRARED OBSERVATIONS

Final Report

May 1980

By: Roy M. Endlich, Senior Research Meteorologist
Daniel E. Wolf, Senior Research Mathematician
Atmospheric Science Center

Prepared for:

National Aeronautics and Space Administration
Goddard Space Flight Center
Greenbelt, Maryland 20771

Attn: Lewis J. Allison, Code 915

Contract NAS5-25730

SRI Project 8600

SRI International
333 Ravenswood Avenue
Menlo Park, California 94025
(415) 326-6200
Cable: SRI INTL MPK
TWX: 910-373-1246

**Technical Report Documentation Page**

| 1. Report No. | 2. Government Accession No. | 3. Recipient's Catalog No. |
|---|---|---|
| | | |

| 4. Title and Subtitle | 5. Report Date |
|---|---|
| Application of an Automatic Cloud Tracking Technique to METEOSAT Water Vapor and Infrared Observations | May 1980 |
| | 6. Performing Organization Code |
| 7. Author(s) Roy M. Endlich, Daniel E. Wolf | 8. Performing Organization Report No. SRI Project 8600 |
| 9. Performing Organization Name and Address<br>SRI International<br>333 Ravenswood Avenue<br>Menlo Park, California 94025 | 10. Work Unit No. (TRAIS) |
| | 11. Contract or Grant No. NAS5-25730 |
| 12. Sponsoring Agency Name and Address<br>National Aeronautics and Space Administration<br>Goddard Space Flight Center<br>Greenbelt, Maryland 20771<br>Lewis J. Allison, Technical Monitor | 13. Type of Report and Period Covered<br>Final Report<br>covering the period<br>5/3/79 through 5/31/80 |
| | 14. Sponsoring Agency Code |

15. Supplementary Notes

16. Abstract

This study applied the SRI automatic cloud tracking system to METEOSAT 6.7-$\mu$m water vapor measurements to learn whether the system can track the motions of water vapor patterns. For experimentation, typical data for the midlatitudes, subtropics, and tropics were selected from a sequence of METEOSAT pictures for 25 April 1978. Trackable features in the water vapor patterns were identified using a clustering technique and the features were tracked by two different methods. In flat (low contrast) water vapor fields, the automatic motion computations were not reliable, but in areas where the water vapor fields contained small-scale structure (i.e., in the vicinity of active weather phenomena) the computations were successful. The tracking results appear to be similar to those obtained by visual analysis of these data. Cloud motions were computed using METEOSAT infrared observations for the same cases (including tropical convective systems and midlatitude jet stream cirrus) and excellent results were obtained.

| 17. Key Words | 18. Distribution Statement |
|---|---|
| Weather satellite data<br>Water vapor patterns<br>Automatic cloud tracking<br>Pattern recognition | |

| 19. Security Classif. (of this report) | 20. Security Classif. (of this page) | 21. No. of Pages | 22. Price |
|---|---|---|---|
| Unclassified | Unclassified | | |

# PREFACE

The SRI International (SRI) automatic tracking system (SATS) computes cloud motion vectors from sequences of observations made by geosynchronous weather satellites. The data used previously in cloud tracking were in the visible and infrared channels as provided by the U.S. Geosynchronous Operational Environmental Satellites (GOES). Recent improvements to the programs have yielded very good results even in cases of complicated multilayer cloud motions (Wolf and Endlich, 1980). The present study under Contract NAS5-25730 applied SATS to water vapor (WV) and infrared (IR) data from the European Space Agency geosynchronous satellite, METEOSAT. METEOSAT obtained sequences of images in the 6.7-μm channel that show water vapor patterns in the middle and upper troposphere. This study investigated the degree to which SATS can operate successfully with these data. For experimentation we selected observations for 25 April 1978 from data furnished by NASA. The regions of interest include portions of the tropics, subtropics, and midlatitudes. We noted that in much of the cloud-free upper atmosphere the water vapor patterns are very "flat" and diffuse. In such regions the automatic target selection identifies small features or gradients as targets and tracks them from frame to frame; however, the accuracy of the results is seriously degraded by noise in the data. We viewed the same data in pictorial form on the SRI cloud console and found that in such cases it is very difficult for a human analyst to discern motions. However, in areas surrounding active weather phenomena (such as the Intertropical Convergence Zone, fronts, and jet streams) the water vapor patterns show small-scale structure outside the cloudy regions; in these areas, automatic water vapor tracking gives reliable results and extends the coverage of motion vectors.

We used two different methods to track the water vapor targets. The MOTION routine matches targets in a manner that minimizes changes in their size, average WV value, and shape and requires that each individual motion conform approximately to the average for the family to which it belongs. The COREL routine makes a cross-correlation computation using a search routine to find the point where a target fits best on a later picture. In flat water-vapor fields, the results of the two methods often disagree, indicating that tracking is unreliable. In fields having small-scale structure, the results of the two methods usually agree; there is a high probability in these cases that the computed motions are correct. We recommend that the automatic method be applied to measurements from the VAS* as soon as these data become available.

We also made automatic computations of cloud motions using the METEOSAT IR data for the same cases, and we consider these results to be very good in regard to accuracy and coverage.

---

*Visible-infrared spin-scan radiometric Atmospheric Sounder.

CONTENTS

ILLUSTRATIONS

# I INTRODUCTION

The automatic tracking system, SATS, developed by SRI International (SRI), computes cloud motion vectors automatically from digital data recorded by geosynchronous weather satellites. The computations are made without operator intervention and are intended to cope with large volumes of data. The system includes steps to select potential targets for tracking in each frame, to identify the same targets in successive frames, and to convert the displacements into motion vectors. The method has been developed and tested using visible and infrared (IR) observations from the Geosynchronous Operational Environmental Satellites (GOES). A description of the automatic tracking has been given previously by Wolf et al.,(1977); the most recent improvements to the techniques have been described by Wolf and Endlich (1980). One improvement involves the enhancement of gradients during the target selection process. This enhancement improves target selection, for example, along the edges of cloud sheets such as cirrus bands. A second improvement minimizes the number of spurious vectors computed near area boundaries, and a third improvement causes the programs to obtain motion vectors in several layers simultaneously. As described by Wolf and Endlich (1980), motion vectors were computed for complicated multilayer clouds associated with Hurricane Eloise using special rapid-scan data for 22 September 1975. We judged the automatically tracked cloud motion vectors to be comparable in number and accuracy to results obtained by human analysts for the same storm (Rodgers et al., 1979). These computer results represent a major improvement over those obtained using earlier versions of SATS, particularly in cases of complex cloud motions.

For a number of years, it has been known that observations in the 6.7-μm channel show water vapor patterns in the upper troposphere and that these patterns are related to air motions (Allison et al., 1971; Steranka et al., 1973); the theoretical possibility of tracking humidity patterns in cloud-free air from sequences of geosynchronous satellite data was discussed by Endlich et al. (1972). The present study for the National Aeronautics and Space Administration (NASA) applied SATS to METEOSAT water vapor (WV) observations, with the specific objective of learning whether the motions can be tracked automatically, particularly in cloud-free regions. Since the water vapor patterns in many regions are "flat" and diffuse (e.g., see Morel et al., 1978) target selection is not a simple matter. We believe that the target-selection process in SATS (Wolf and Endlich, 1980) performs well. Different methods for identifying targets have been used by Kaestner and Fischer (1980) with Nimbus 5 data. They used a gradient operator and an edge detection algorithm and tracked the resulting targets by eye, obtaining good results.

SATS has the ability to track automatically selected targets in two independent ways: using the MOTION routine (which matches targets so as

to minimize changes in size, average WV value, and shape), and using the COREL routine (which makes a cross-correlation computation). The MOTION routine matches each group at time 1 with its best likeness (in terms of size, WV value, IR value, and shape) at time 2, and requires that the potential motion vector conform approximately to the average motion of the family to which it belongs. The COREL routine makes a cross-correlation computation using a search routine to find the point where a target at time 1 fits best at time 2 (see Wolf and Endlich, 1980). In both the MOTION and COREL routines, the average layer motion computed for the first picture pair of a series is used as a first guess for the second pair, and so on throughout the series. This practice tends to introduce continuity in a series of computed motion vectors.

This study used both routines and compared them; consistency of their results was a requirement for accuracy. We viewed the data in pictorial form on the SRI cloud console in a manner analogous to cloud tracking on the Atmospheric and Oceanographic Information Processing System (AOIPS) as described by Hasler et al. (1976). We evaluated the automatic computations qualitatively and determined the extent to which WV motions could be identified by a human analyst through visual study.

## II DATA ANALYSIS

A series of METEOSAT images obtained at 30-minute intervals on 25 April 1978 by the European Space Center was furnished to us on magnetic tape by NASA. The visible channel is blank because the data were taken at night. The IR and WV data were recorded at a nominal resolution of 5 km. We selected four tapes at 0030, 0100, 0130, and 0200 GMT for purposes of experimentation. These data are part of a series covered in a motion picture film, made by the European Space Agency, that was furnished to us by NASA. We used it to aid in evaluating the computed motions of WV patterns and clouds.

Initial inspection of some samples of METEOSAT observations indicated that there was random unevenness that might be caused by instrumental noise. Partly for this reason, and because we wanted to be able to measure high-speed (e.g., jet stream) motions, we averaged the original 5-km data to a resolution of 10 km. With 30-minute data, 10-km resolution keeps the displacements within the search radius of the MOTION program; 5-km data might not. Figure 1 shows the full-disk WV image of the earth at the beginning of the series of pictures used in this study; Figure 2 shows the corresponding IR image.

The computer program for reading the METEOSAT data tapes is written to invert the numbering of rows and columns, so that the coordinates used in selecting areas will be analogous to those for GOES data. [The METEOSAT rows (scan lines) are numbered from south to north, and columns are numbered from east to west, opposite to the convention of U.S. satellites.]

In the usual images of satellite data, clouds are bright in the visible channel, cold areas are bright in IR data, and moist areas are bright in WV data. However, to emphasize the dry areas in some of the WV images shown later, we have reversed the values so that dry areas are bright. This is done simply by changing the WV values to (256 - WV). Since WV patterns are continuous (in contrast to the discontinuous nature of clouds), one can select for tracking WV targets that are either relatively moist or relatively dry compared with their local surroundings. An option has been introduced in the program to select the preferred mode. We tested both options but did not find any advantage of one over the other.

For purposes of experimentation we selected data for a north-south swath starting in the northwestern part of the image of Figure 1 and extending to the southwestern part. This swath extends from the Northern Hemisphere midlatitudes across the equator to the Southern Hemisphere midlatitudes and includes a wide variety of weather and cloud patterns. The swath is divided into areas of 70 by 120 pixel units of 10-km resolution, so each area covers approximately 700 by 1200 km.

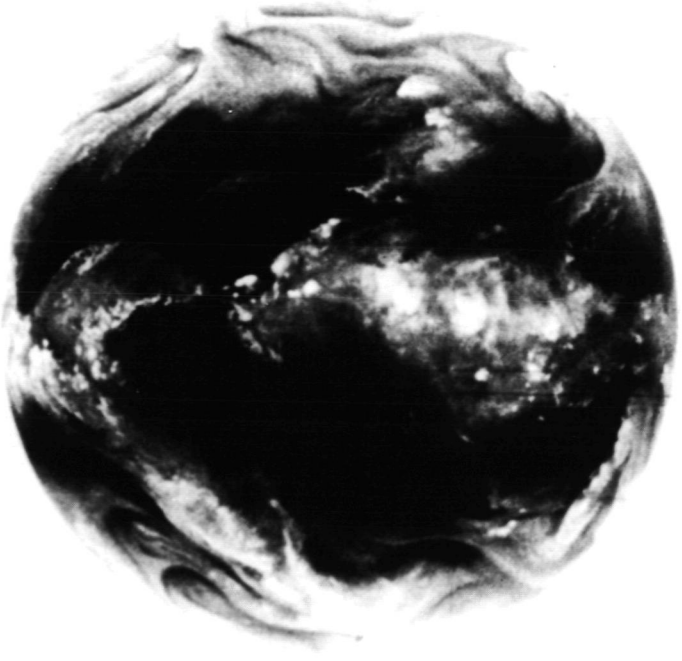

FIGURE 1 FULL DISK IMAGE OF METEOSAT WATER VAPOR DATA FOR 0030 GMT, 25 APRIL 1978

The center of the picture lies on the equator at the Greenwich meridian.

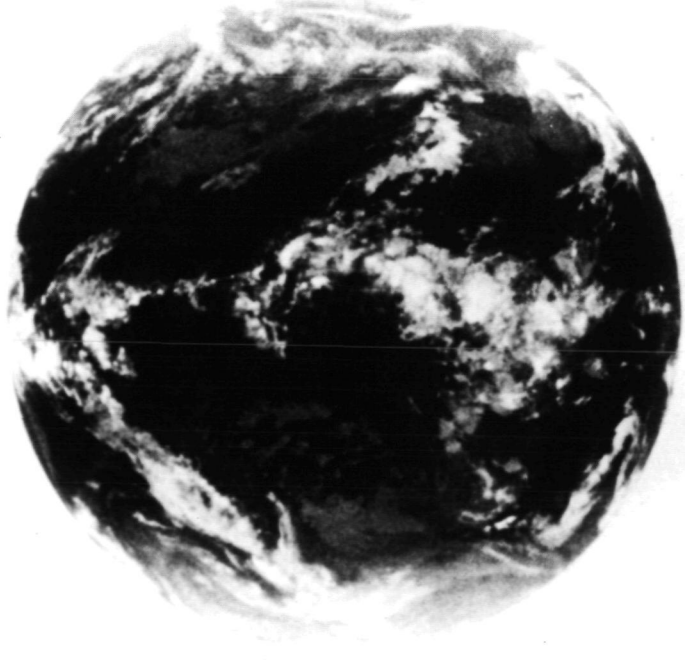

FIGURE 2 FULL DISK IMAGE OF METEOSAT INFRARED DATA CORRESPONDING TO FIGURE 1

## III OBJECTIVE MOTION COMPUTATIONS

This section will show typical computations for the tropics, subtropics, and midlatitudes. The first area lies along the north side of the Intertropical Convergence Zone (ITCZ) and includes part of the northwestern African coast near the eastern border. Figure 3 shows the WV data for this area, and Figure 4 shows the IR image. The African coast cannot be seen in Figure 4 because the nighttime land and water temperatures are nearly the same. (These figures, and similar ones in this report, were generated from the digital METEOSAT data using the SRI CDC-280 CRT display system.) Where the clouds penetrate into the upper troposphere, the WV and IR patterns are quite similar. Both images have distinct features when viewed in this pictorial form. The motions computed for WV targets selected automatically from Figure 3 and the three subsequent pictures are shown in Figure 5. There are three picture pairs for the four tapes. It can be seen in Figure 5 that some targets were tracked in all three picture pairs, some in two picture pairs, and some in only one. There is a consistent pattern of motions. The numbers beside each vector refer to the average value of the IR data for the target. The four categories used are for IR values less than 100, from 100 to 140, from 140 to 180, and greater than 180; these categories were previously selected from GOES IR data to separate clouds into categories of low, middle, high, and deep convective. For METEOSAT IR data the IR range is different; category 1 (IR values less than 100) is seldom observed; category 2 refers to low clouds; category 3 to middle clouds; and category 4 to high or deep convective clouds. When tracking is done using WV data, the value of the associated IR data is an approximate indicator of the height of the clouds at that point, but it has little relation to the height of the water vapor motion vectors. Therefore, in Figure 5 and in subsequent plots of water vapor pattern motions, the height indicators can be disregarded.

The pattern of motions in Figure 5 shows a drift toward the north. The average speed of the WV motion vectors is 6 $ms^{-1}$. We have verified this pattern by inspecting the data visually using an animated sequence on the SRI cloud console (Serebreny et al., 1970). In this case, where the WV pattern (Figure 3) has distinct features, the automatic tracking is successful. The results of tracking the WV pattern using the COREL routine are shown in Figure 6. Some vectors disagree with their neighbors in speed or direction and therefore appear spurious, but the results are otherwise in reasonably good agreement with Figure 5.

The results of tracking the IR patterns using the MOTION routine are shown in Figure 7; results using the COREL routine are shown in Figure 8. Here the height indicators can be used to distinguish the approximate cloud altitudes in the manner mentioned earlier. The patterns of Figure 7 and Figure 8 are each reasonably consistent internally,

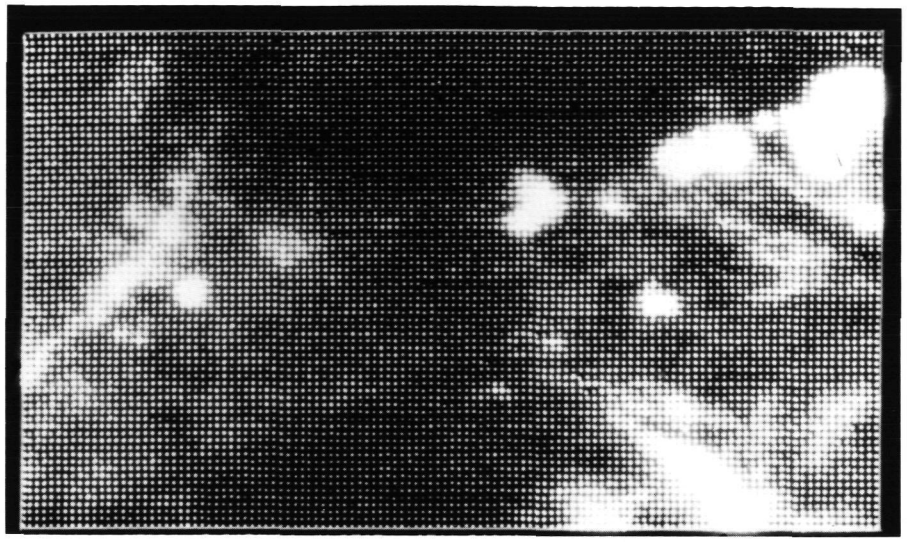

FIGURE 3 IMAGE OF 10-KM RESOLUTION WATER VAPOR DATA FOR AN AREA ALONG THE NORTHERN SIDE OF THE INTERTROPICAL CONVERGENCE ZONE

The area measures approximately 700-km north/south and 1200-km east/west

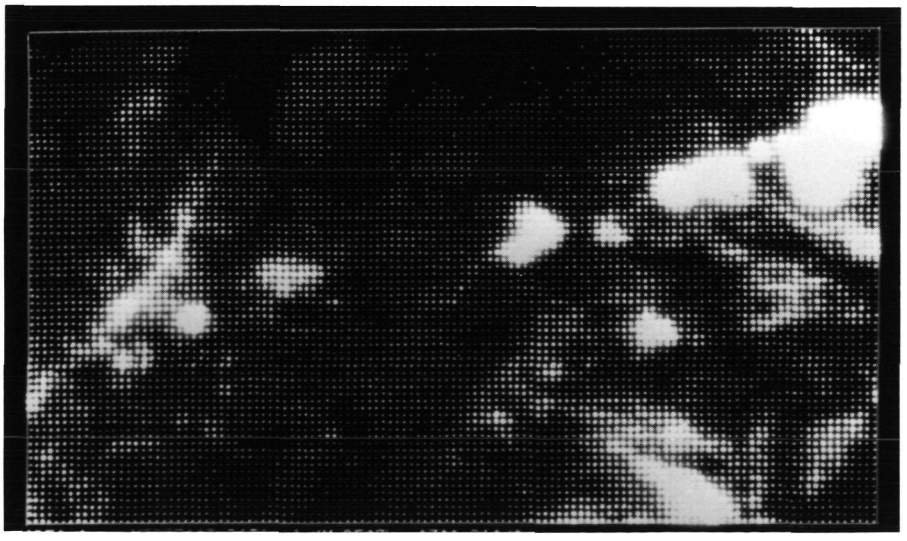

FIGURE 4 IMAGE OF 10-KM RESOLUTION INFRARED DATA CORRESPONDING TO FIGURE 3

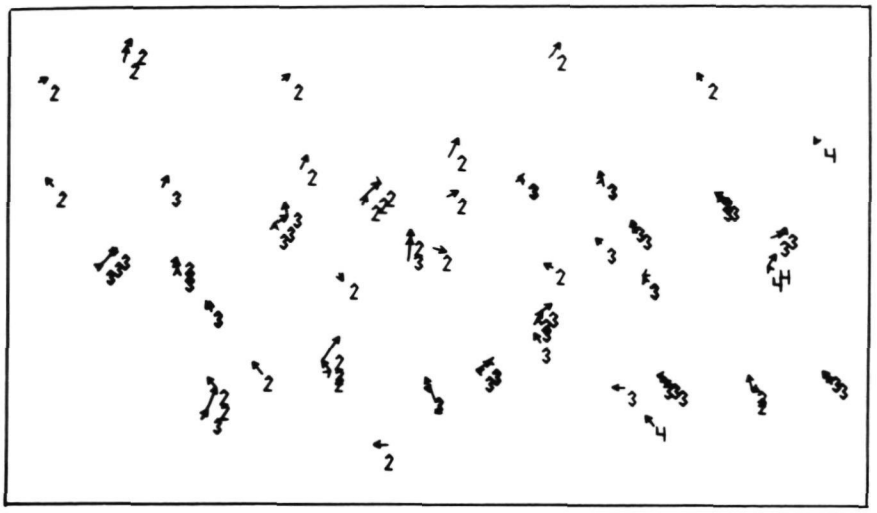

FIGURE 5 MOTION VECTORS OF WATER VAPOR PATTERNS FOR THREE PICTURE PAIRS FOR THE AREA OF FIGURE 3 COMPUTED USING THE MOTION ROUTINE

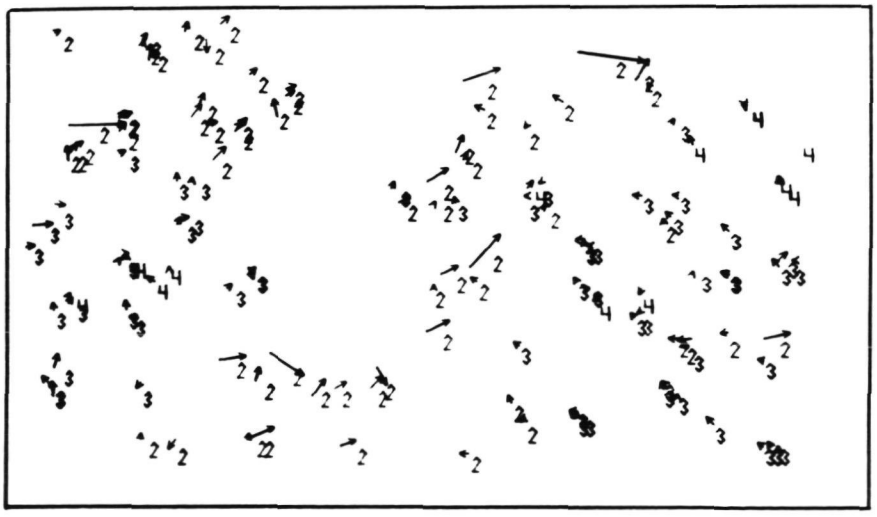

FIGURE 6 MOTION VECTORS OF WATER VAPOR PATTERNS CORRESPONDING TO FIGURE 5 COMPUTED USING THE COREL ROUTINE

FIGURE 7 CLOUD MOTIONS COMPUTED FROM INFRARED DATA FOR THREE PICTURE PAIRS FOR THE AREA OF FIGURE 4 USING THE MOTION ROUTINE

FIGURE 8 CLOUD MOTIONS CORRESPONDING TO FIGURE 7 COMPUTED USING THE COREL ROUTINE

and the two figures agree well with each other. As the programs currently exist, the MOTION routine ignores targets that are too changeable in size, IR value, WV value or displacement to be reliable. However the COREL routine does not have this feature; it computes motions for all targets. Therefore the density of vectors is greater in Figure 6 than in Figure 5 and greater in Figure 8 than in Figure 7.

The WV and IR data for the subarea directly south of Figures 3 and 4 are shown in Figures 9 and 10. The equator passes approximately through the middle of this area. The WV and IR data have similar patterns: The WV pattern is very flat (lacks contrast) in the southwestern part of the area. The WV movements computed by the MOTION routine for the three picture pairs are shown in Figure 11. There is flow from the eastnortheast in the vicinity of the convective cells. Only a few vectors are obtained in the flat part of the pattern. The vectors computed for the same data using the COREL routine are shown in Figure 12. The pattern is similar to Figure 11 in the eastern part of the region, but the motions are opposite in the western part. We studied the motions visually using the cloud console but could not discern which computations are more nearly correct. The National Meteorological Center (NMC) 500-mb analysis indicates very weak flow in this region. This uncertainty illustrates the difficulty of making judgments of computations for regions of flat WV patterns.

The cloud motions computed from the IR data using the MOTION routine and the COREL routine are shown in Figures 13 and 14 respectively. The pattern in Figure 13 is entirely consistent and agrees with visual studies of these IR data on the cloud console. Figure 14 contains a few spurious vectors that disagree with nearby neighbors, but the pattern is acceptable and the coverage is good.

The northern boundary of the next area to be discussed begins approximately 700-km south of the southern boundary of Figures 9 and 10 and is typical of subtropical high-pressure regions. The WV and IR data are shown in Figures 15 and 16. Except in the southwest corner, the WV pattern is very flat, whereas the IR data show patchy low clouds. The automatic target selection process identified minor features of Figure 15 as targets and tracked them, as shown in Figure 17. Only one target was tracked for all three picture pairs. The results of WV tracking using the COREL routine are shown in Figure 18. There is generally a pattern of eastward vectors (with some local disagreements), and the general result is almost opposite to that of Figure 17. Use of the cloud console to study the WV data does not reveal any clear pattern of motions to the eye. The NMC 500-mb analysis for this region (obtained from the National Climatic Center) shows a weak flow from the west and indicates that Figure 18 rather than Figure 17 is more nearly correct for this very flat WV pattern. We believe that in a field of such flatness, the target selection and tracking routines become significantly affected by noise in the measurements; with the IR data, noise is much less important.

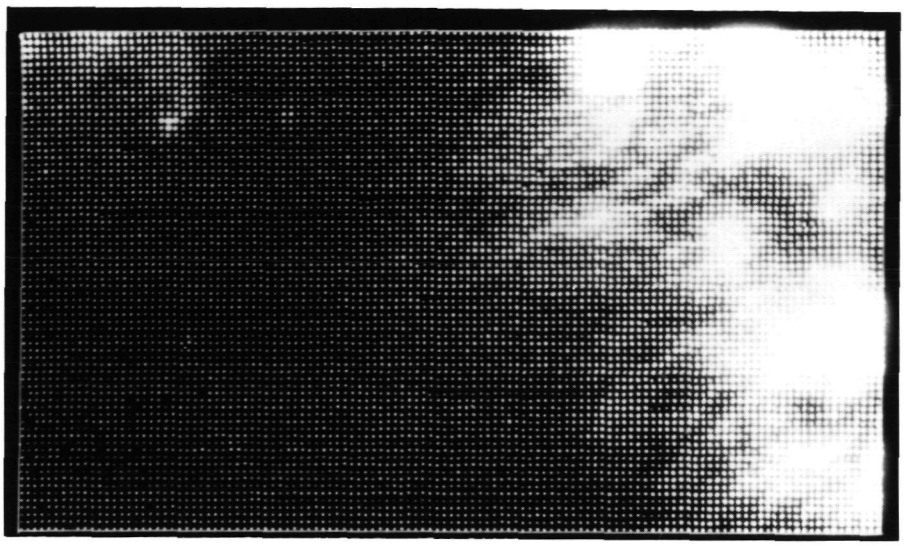

FIGURE 9 IMAGE OF 10-KM RESOLUTION WATER VAPOR DATA FOR AN EQUATORIAL AREA LYING DIRECTLY SOUTH OF FIGURE 3

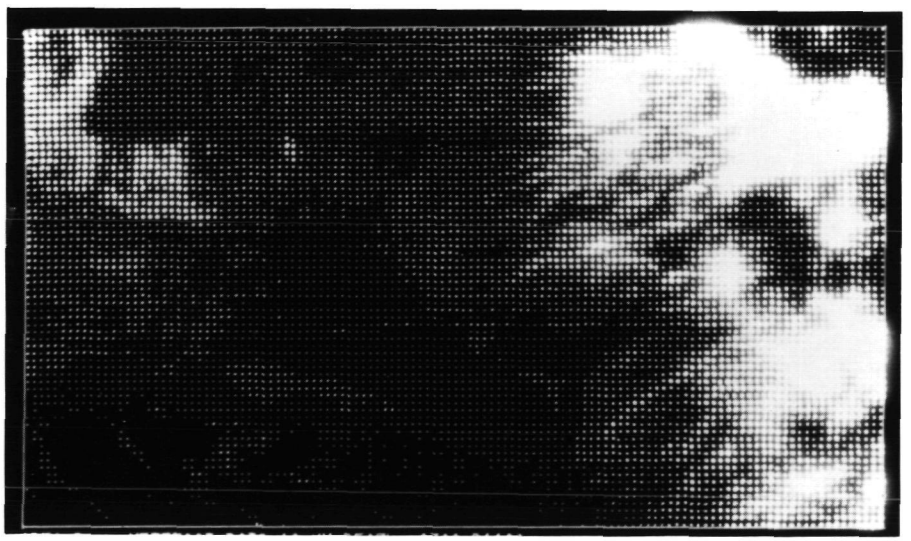

FIGURE 10 IMAGE OF 10-KM RESOLUTION INFRARED DATA CORRESPONDING TO FIGURE 9

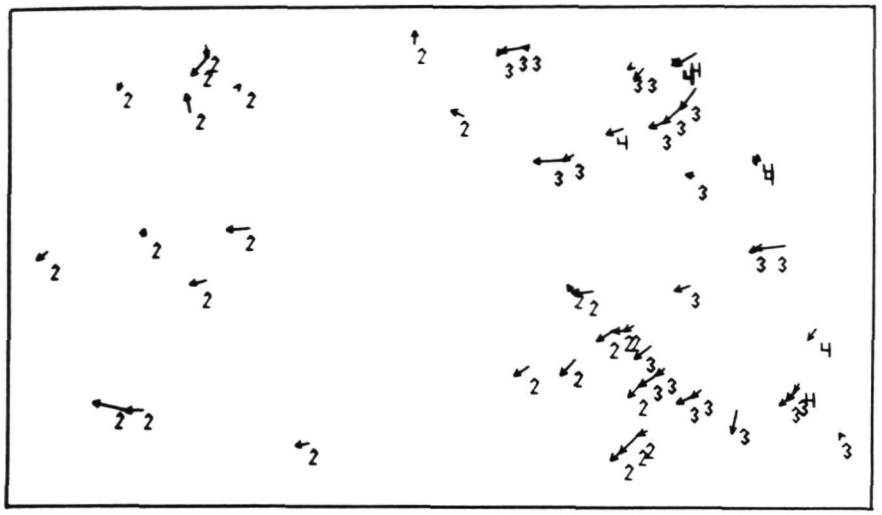

FIGURE 11 MOTION VECTORS OF WATER VAPOR PATTERNS FOR THREE PICTURE PAIRS FOR THE AREA OF FIGURE 9 COMPUTED USING THE MOTION ROUTINE

FIGURE 12 MOTION VECTORS OF WATER VAPOR PATTERNS CORRESPONDING TO FIGURE 11 COMPUTED USING THE COREL ROUTINE

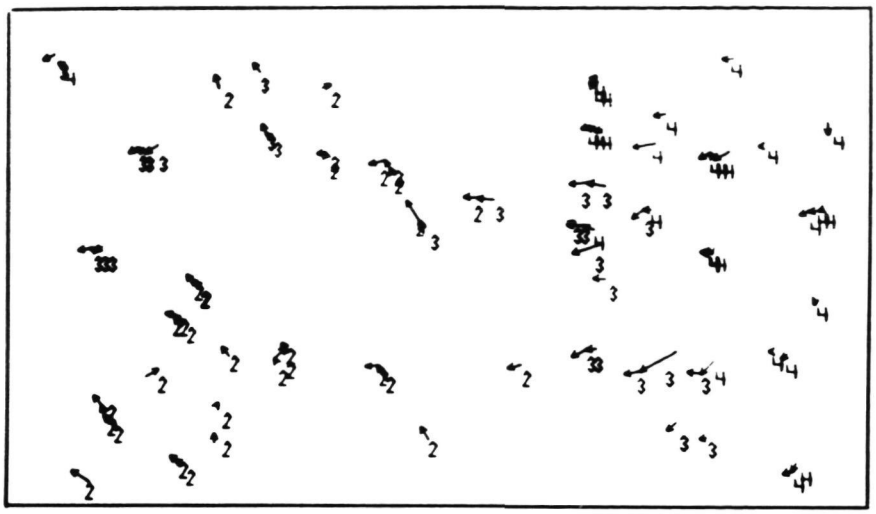

FIGURE 13 CLOUD MOTIONS COMPUTED FROM INFRARED DATA FOR THREE PICTURE PAIRS FOR THE AREA OF FIGURE 10 COMPUTED USING THE MOTION ROUTINE

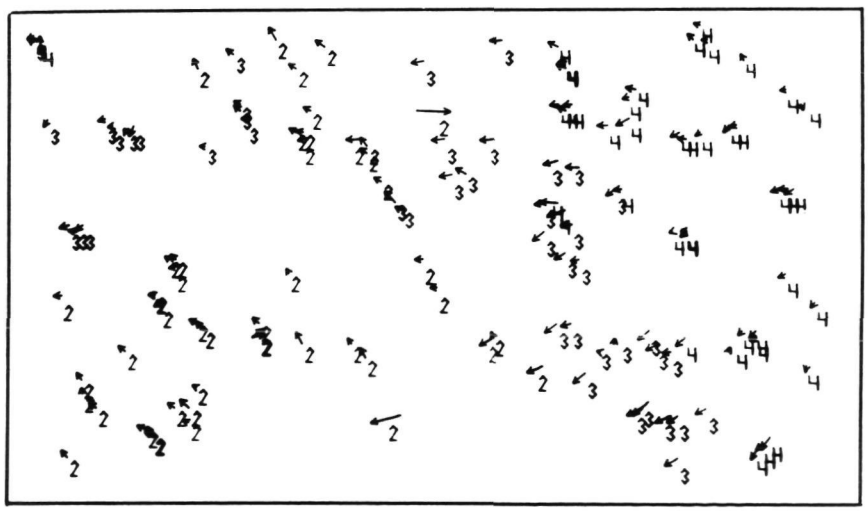

FIGURE 14 CLOUD MOTIONS CORRESPONDING TO FIGURE 13 COMPUTED USING THE COREL ROUTINE

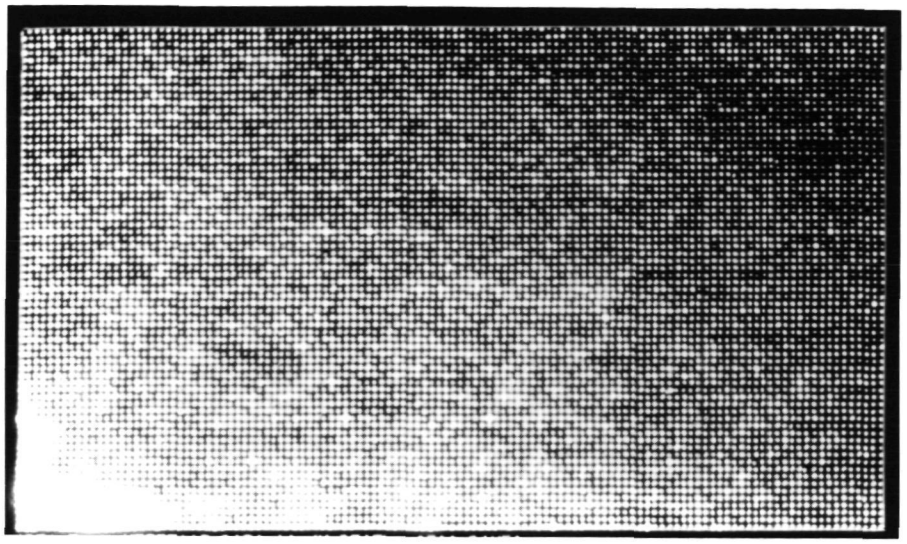

FIGURE 15 IMAGE OF 10-KM RESOLUTION WATER VAPOR DATA FOR A SUBTROPICAL AREA LYING 700-KM SOUTH OF FIGURE 9, SHOWING A VERY FLAT, DIFFUSE PATTERN

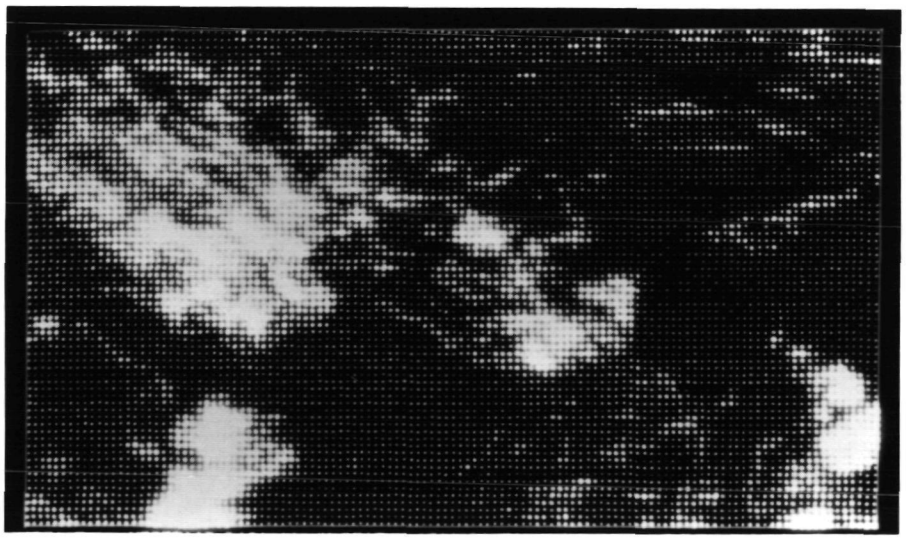

FIGURE 16 IMAGE OF 10-KM RESOLUTION INFRARED DATA CORRESPONDING TO FIGURE 15

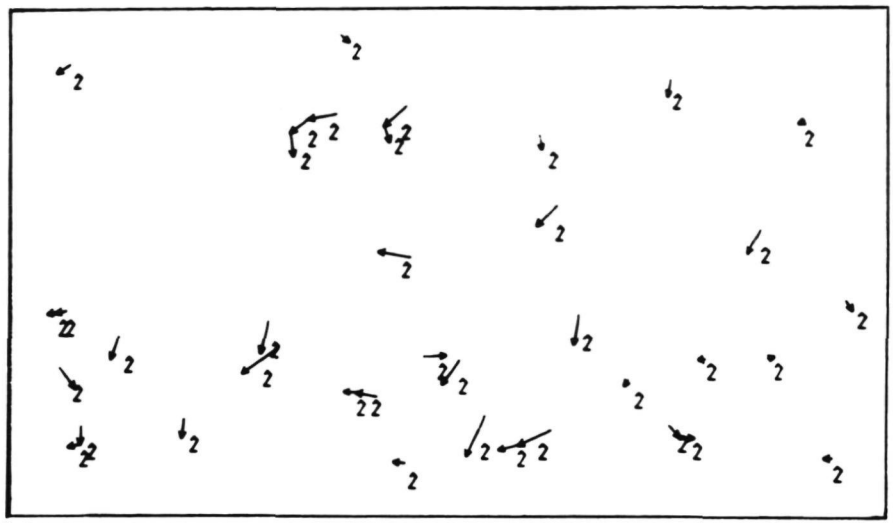

FIGURE 17 MOTION VECTORS OF WATER VAPOR PATTERNS FOR THREE PICTURE PAIRS FOR THE AREA OF FIGURE 15 COMPUTED USING THE MOTION ROUTINE

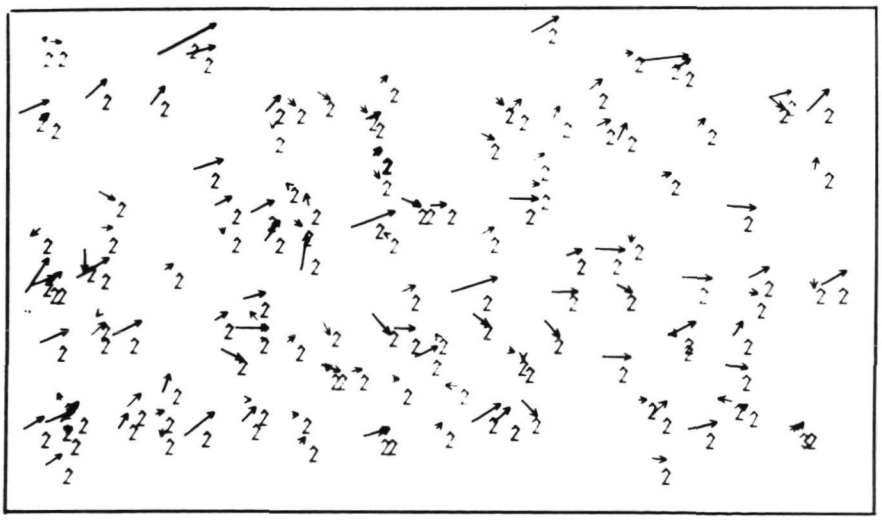

FIGURE 18 MOTION VECTORS OF WATER VAPOR PATTERNS CORRESPONDING TO FIGURE 17 COMPUTED USING THE COREL ROUTINE

The cloud tracking using the IR data is shown in Figure 19 for the MOTION routine and in Figure 20 for the COREL routine. The patterns of low cloud motions in Figure 19 agree well with motions seen visually using the cloud console. Figure 20 has more vectors, including a few spurious ones, but is in good agreement with Figure 19.

The northern edge of the next area to be discussed is located approximately 700-km south of the southern boundary of Figures 15 and 16. The WV and IR data for this midlatitude area are shown in Figures 21 and 22. Here the WV image is reversed in regard to black and white; in contrast to previous figures, dry areas appear white. The WV pattern has distinct structure in the southwest corner and rather flat patterns elsewhere, but it is not as featureless as in Figure 15. The IR pattern shows the edge of a cirrus band (clearly visible in the southwestern part of Figure 2) in the southwest corner. The motion of the targets in the water vapor patterns are shown in Figure 23; the predominant motion is toward the east. The WV motions computed using the COREL routine are shown in Figure 24, again indicating motion toward the east. When viewed on the cloud console the pattern motion toward the east is verified, and the NMC 500-mb analysis shows eastward motions. In the southwest corner, the cirrus band is moving rapidly toward the eastsoutheast, not from the north as shown in Figure 23.

The results of tracking IR targets using the MOTION routine and the COREL routine are shown in Figures 27 and 28. Figure 25 shows rapid motion of the cirrus band (the average of the Layer 4 motions is 295°, 30 $ms^{-1}$) and consistent motion of the middle clouds (Layer 3) from the east. The motions of the middle clouds and the WV motions are apparently in opposite directions. (It is worth remembering that motions in various layers are computed simultaneously in these routines.) The motions computed by cross correlation (Figure 26) show the same pattern as Figure 25, except for a few spurious vectors.

The last area to be discussed lies just south of Figures 21 and 22 and is shown in Figures 27 and 28. In Figure 27 the WV data are in the reversed form such that dry areas appear white. There is very distinct structure in the field, mostly attributable to the presence of high clouds. The IR data (Figure 28) show the cirrus band and some lower clouds. In Figures 1 and 2, this cirrus band can be seen originating in the Amazon basin and extending to the southeast for a very long distance. It is one of the most striking features to be seen in the film (mentioned earlier) of METEOSAT data for this date. The motions of WV targets computed using the MOTION routine are shown in Figure 29. The speeds measured within the cirrus band in the southwestern part of the area are as large as 68 $ms^{-1}$; however, they were computed without the use of a first guess. In this region the NMC 500-mb analysis shows an isotach center with wind speeds to 55 knots (28 $ms^{-1}$). Probably the cirrus were in the 300- to 250-mb layer, where winds were stronger than below.

It is interesting that motions are computed in the water vapor patterns outside the cirrus band as shown in the IR data. These motions

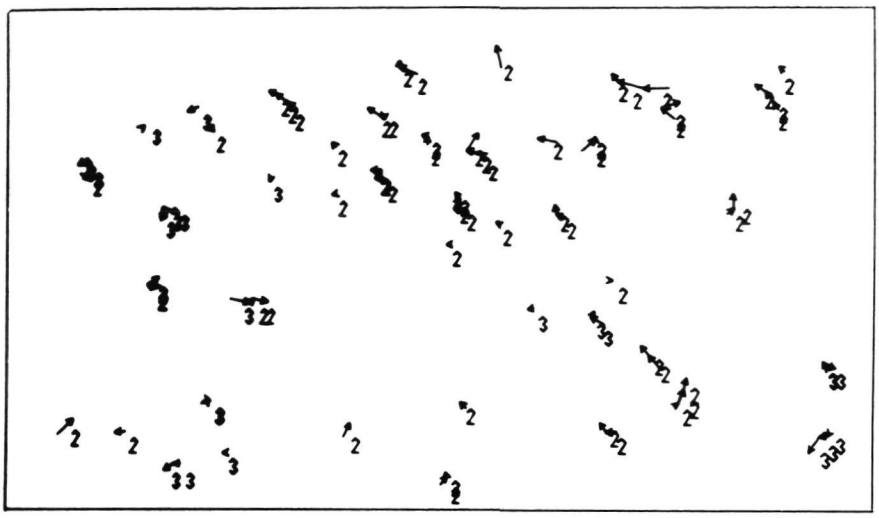

FIGURE 19 CLOUD MOTIONS COMPUTED FROM INFRARED DATA FOR THREE PICTURE PAIRS FOR THE AREA OF FIGURE 16 USING THE MOTION ROUTINE

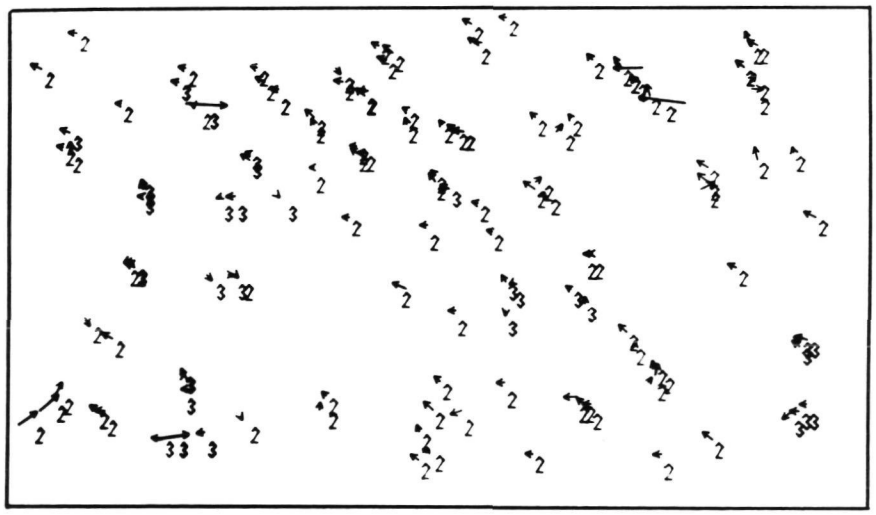

FIGURE 20 CLOUD MOTIONS CORRESPONDING TO FIGURE 19 COMPUTED USING THE COREL ROUTINE

FIGURE 21 IMAGE OF 10-KM RESOLUTION WATER VAPOR DATA FOR A MIDLATITUDE AREA LYING 700-KM SOUTH OF FIGURE 15

Moist areas are dark, dry areas are white.

FIGURE 22 IMAGE OF 10-KM RESOLUTION INFRARED DATA CORRESPONDING TO FIGURE 21

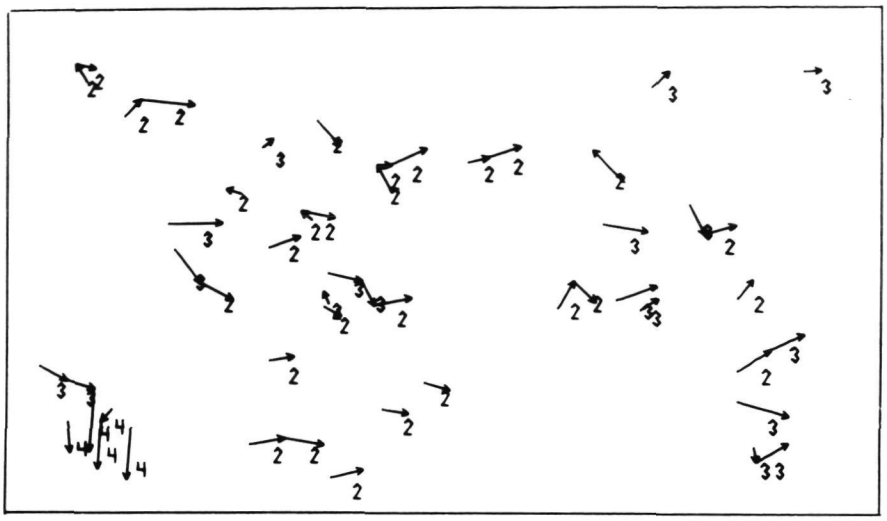

FIGURE 23 MOTION VECTORS OF WATER VAPOR PATTERNS FOR THREE PICTURE PAIRS FOR THE AREA OF FIGURE 21 COMPUTED USING THE MOTION ROUTINE

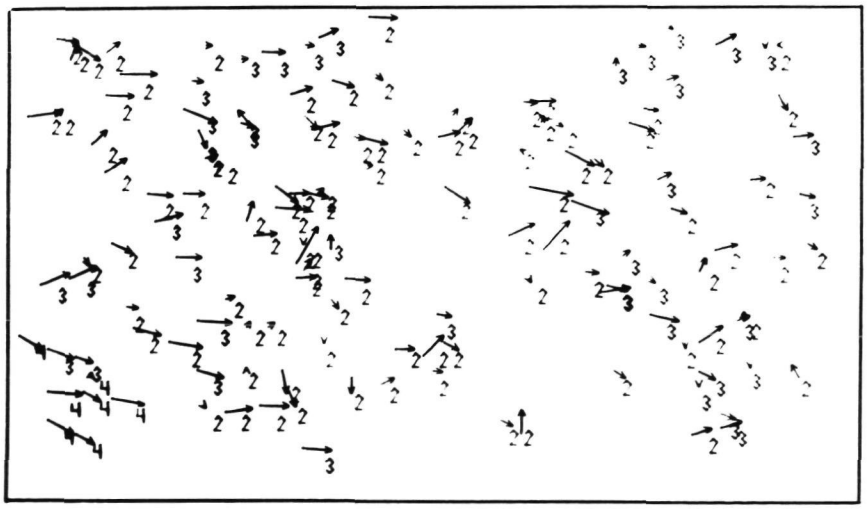

FIGURE 24 MOTION VECTORS OF WATER VAPOR PATTERNS CORRESPONDING TO FIGURE 23 COMPUTED USING THE COREL ROUTINE

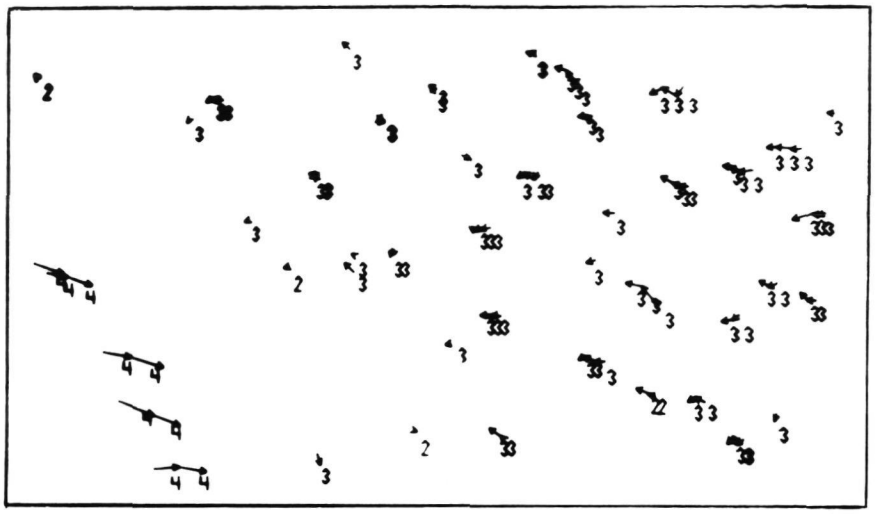

FIGURE 25 CLOUD MOTIONS COMPUTED FROM INFRARED DATA FOR THREE PICTURE PAIRS FOR THE AREA OF FIGURE 22 USING THE MOTION ROUTINE

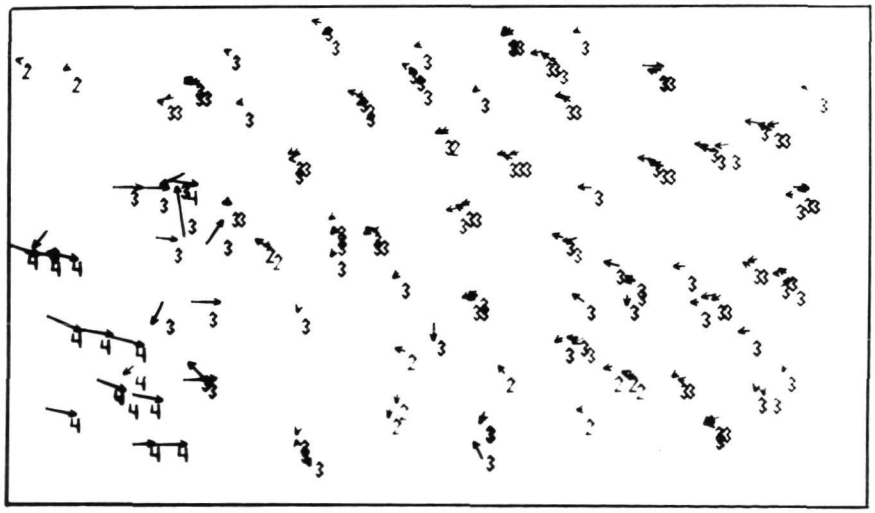

FIGURE 26 CLOUD MOTIONS CORRESPONDING TO FIGURE 25 COMPUTED USING THE COREL ROUTINE

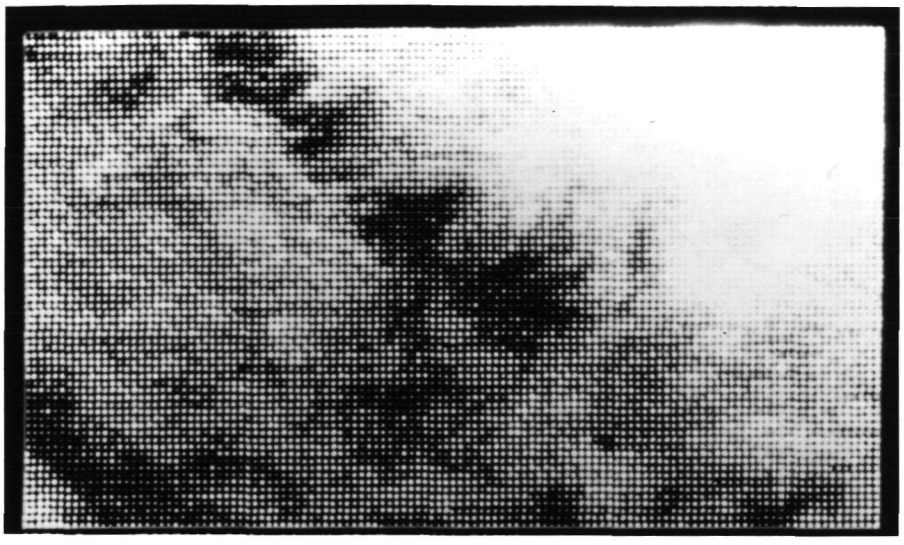

FIGURE 27 IMAGE OF 10-KM RESOLUTION WATER VAPOR DATA FOR A MIDLATITUDE AREA LYING DIRECTLY SOUTH OF FIGURE 21 CONTAINING A JET STREAM CIRRUS BAND

Moist areas are dark, dry areas are white.

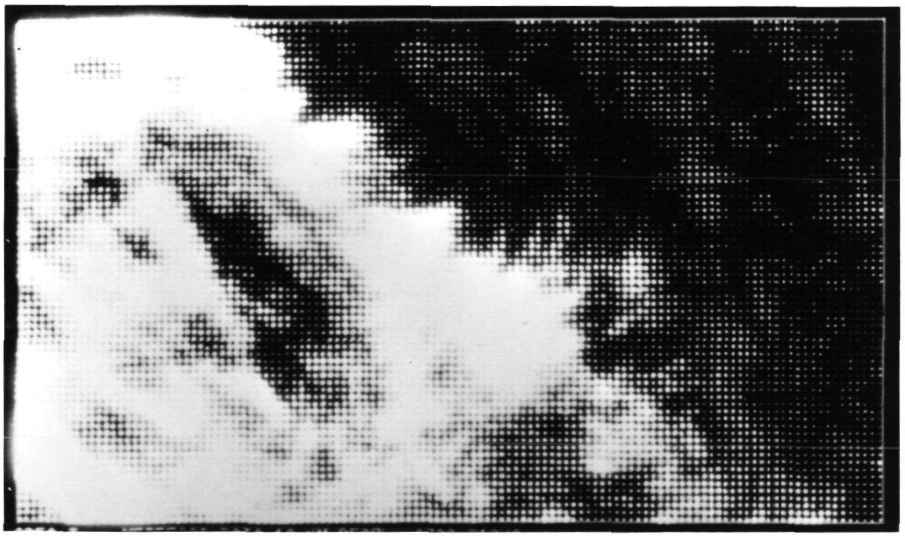

FIGURE 28 IMAGE OF 10-KM RESOLUTION INFRARED DATA CORRESPONDING TO FIGURE 27

verify very well when the data are viewed on the cloud console. The corresponding motions computed by cross correlation are shown in Figure 30. The results are not reliable within the highest speed flow of the cirrus band, probably because the searching over relatively large distances that was done in the correlation routine became confused. However, the motions are generally satisfactory above a line running from the southeast corner to the northwest corner of the area. The motions of IR targets computed by the MOTION routine and the COREL routine are shown in Figures 31 and 32. In Figure 31, a number of targets are tracked in all three picture pairs. The computed motions of both the cirrus band and the middle clouds are verified when the images are viewed using the cloud console. In Figure 32 the COREL routine gives some spurious vectors for the IR targets, but the overall results are good.

To determine whether WV pattern tracking would be facilitated by using data of coarser resolution, we carried out a single experiment using original data averaged to 30-km resolution for four images at hourly intervals. The region selected (approximately 2100 by 3600 km) extended from the ITCZ northward. The results were similar to those reported earlier; i.e., the WV and IR tracking were successful in and around the active weather phenomena, but in the areas of low moisture (and low contrast) only a few useful motions were obtained.

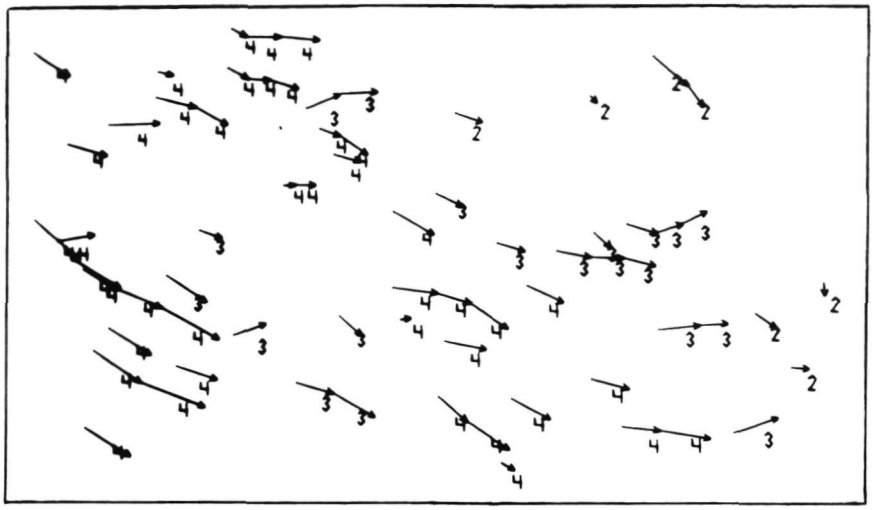

FIGURE 29 MOTION VECTORS OF WATER VAPOR PATTERNS FOR THREE PICTURE PAIRS FOR THE AREA OF FIGURE 27 COMPUTED USING THE MOTION ROUTINE

FIGURE 30 MOTION VECTORS OF WATER VAPOR PATTERNS CORRESPONDING TO FIGURE 29 COMPUTED USING THE COREL ROUTINE

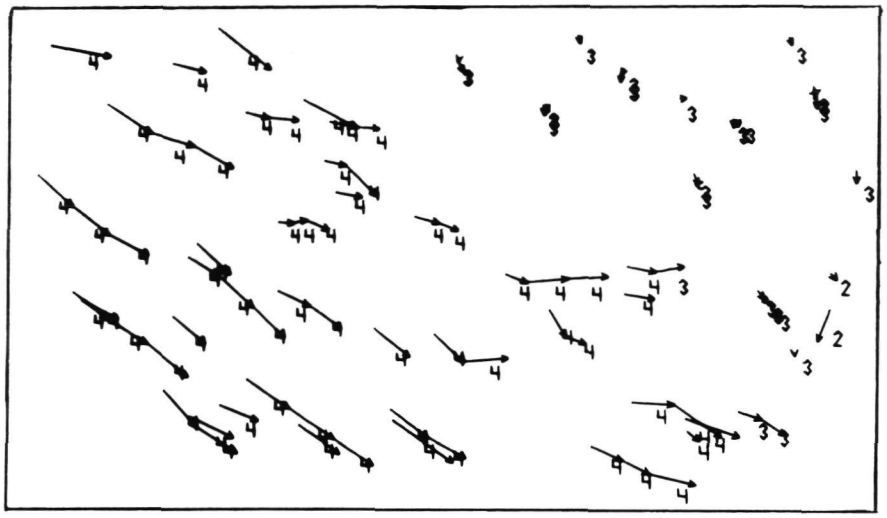

FIGURE 31 CLOUD MOTIONS COMPUTED FROM INFRARED DATA FOR THREE PICTURE PAIRS FOR THE AREA OF FIGURE 28 USING THE MOTION ROUTINE

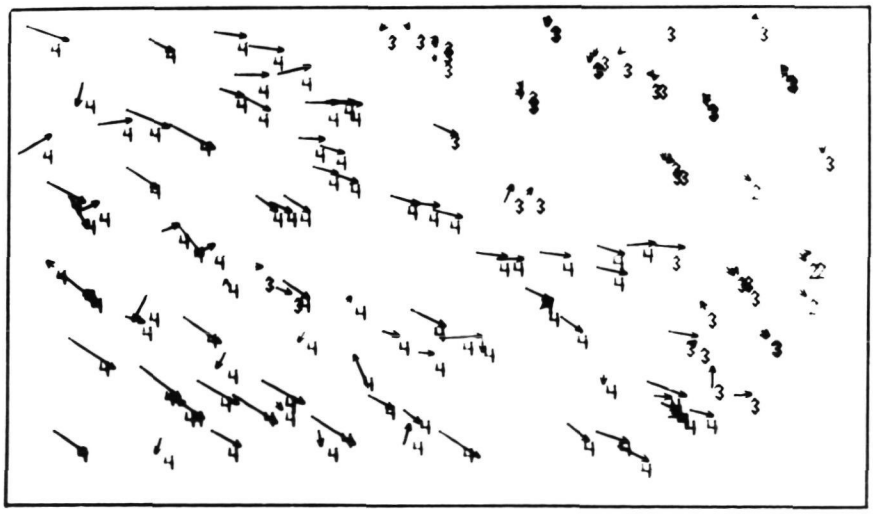

FIGURE 32 CLOUD MOTIONS CORRESPONDING TO FIGURE 31 COMPUTED USING THE COREL ROUTINE

# IV CONCLUSIONS

We have established that automatic tracking of METEOSAT WV patterns is feasible in those areas where the patterns have structure sufficiently detailed that tracking by present visual methods is feasible.

Our computations show that SATS identifies potential targets even where the WV fields are very flat (lack contrast). However, in these flat fields both target selection and tracking are believed to be significantly degraded by noise in the observations. The data for 25 April 1978 indicate that the areas of flat water vapor patterns constitute roughly half of the potential tracking area within the field of view of METEOSAT. Other pictorial data that we have inspected indicate that flat fields may be less extensive; further investigation of their prevalence is needed.

It would be desirable to determine in advance whether WV tracking is feasible in a particular area. From present experience, we believe that a type of histogram analysis could be devised to give a reliable indication. For example, the histogram of WV values for the flat field of Figure 15 is shown by the dashed line in Figure 33: It is strongly peaked and covers only part of the range. The histogram for Figure 3, which had distinct WV patterns and provided satisfactory tracking results, is broader as shown by the solid line in Figure 33. Thus, a measure of the peakedness and spread of the histogram for an area should indicate whether valid tracking is to be expected by applying SATS to METEOSAT data. Another way to determine the reliability of automatically computed motions of water vapor patterns would be to make computations using both the MOTION and COREL routines, as we have done. Our experience indicates that where the results agree, the computations have a high probability of being reliable, but this is counterbalanced by the expense of making two sets of computations.

The cases that we have studied indicate that WV patterns suitable for tracking extend outward from the edges of cloud phenomena such as the ITCZ, fronts, and jet streams. Within the cloud bands, WV tracking has no apparent advantage over IR tracking, but along the edges of the clouds some additional motions may be determined from the WV data. As a result of visual study of the METEOSAT WV patterns and a preliminary computation, we suspect that WV tracking may be more feasible for data of larger scale and coarser resolution than the 10-km resolution data we used. Data of 20- to 30-km resolution at 1- to 2-hour intervals might be suitable for computing synoptic scale pattern motions.

In the cloud motions computed using METEOSAT IR data, we believe that all of the results are reliable. Where the displacements are

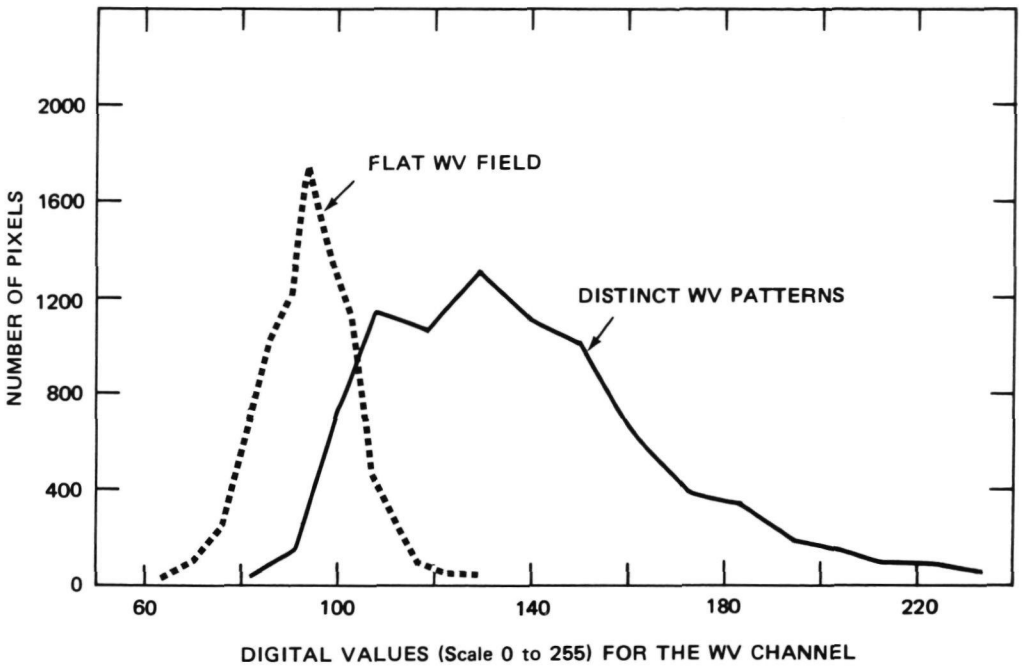


FIGURE 33 HISTOGRAMS OF WATER VAPOR FOR THE EQUATORIAL AREA OF FIGURE 3 (SOLID) AND FOR THE SUBTROPICAL AREA OF FIGURE 15 (DASHED)

relatively large in the time interval between pictures, the MOTION routine appears to give fewer erroneous vectors than the COREL routine, but the COREL routine gives a higher density of motions.

We conclude that tracking METEOSAT WV patterns using SATS is subject to approximately the same limitations as apply in human tracking of the same data. Further improvements in operational WV data, for example from the VAS sensor, may increase the effectiveness of WV tracking. Similarly, further improvements in automatic tracking methods such as SATS may lead to better results.

We recommend that further tracking experiments be performed by appling SATS to METEOSAT data and to VAS data, as soon as the latter become available. Tracking results obtained by SATS, by the methods of Kaestner and Fischer (1980), and using consoles, such as AOIPS (Hasler et al., 1976) and McIdas (Smith, 1975) should be compared.

## REFERENCES


Allison, L. J., J. Steranka, G. T. Cherrix, and E. Hilsenrath, 1972: Meteorological applications of the Nimbus 4 temperature-humidity radiometer, 6.7 micron channel data. Bull. Amer. Meteor. Soc., 53, 526-535.

Endlich, R. M., R. L. Mancuso, and R. E. Nagle, 1972: A proposed method for determining winds in cloud-free regions by isentropic analysis of temperature and water vapor profiles. J. Appl. Meteor., 11, 1019-1021.

Hasler, A. F., W. Shenk, and J. P. Gary, 1976: A study of a STORMSAT interactive data analysis facility. Preprints, Seventh Conf. Aerospace and Aeronautical Meteorology, Melbourne, Amer. Meteor. Soc., 284-290.

Kaestner, M., and H. Fischer, 1980: Wind determination from Nimbus 5 observations in the 6.3 μm water vapor band. J. Appl. Meteor. (in press).

Morel, P., M. Desbois, and G. Szejwach, 1978: A new insight into the troposphere with the water vapor channel of METEOSAT. Bull. Amer. Meteor. Soc., 59, 711-714.

Rodgers, E., R. C. Gentry, W. Shenk, and V. Oliver, 1979: The benefits of using short-interval satellite images to derive winds for tropical cyclones. Mon. Wea. Rev., 107, 575-584.

Serebreny, S. M., E. J. Weigman, R. G. Hadfield, and W. E. Evans, 1970: Electronic system for utilization of satellite cloud pictures. Bull. Amer. Meteor. Soc., 51, 848-855.

Smith, E., 1975: Man-computer interactive data access system. IEEE Trans. Geosci. Electron., GE-13, 123-126.

Steranka, J., L. J. Allison, and V. V. Salomonson, 1973: Application of Nimbus 4 THIR 6.7 μm observations to regional and global moisture and wind field analysis. J. Appl. Meteor., 12, 386-395.

Wolf, D. E., D. J. Hall, and R. M. Endlich, 1977: Experiments in automatic cloud tracking using SMS-GOES data. J. Appl. Meteor., 16, 1219-1230.

Wolf, D. E., and R. M. Endlich, 1980: Application of the SRI cloud tracking technique to rapid-scan GOES observations. Final Report, Contract NAS 5-25027, SRI International, Menlo Park, California, 26 pp.